Planetary backup bearings for high speed applications and service life estimation Methodology

Lukas QUURCK*, Benedikt SCHUESSLER, Daniel FRANZ, Stephan RINDERKNECHT

* Institute for Mechatronic Systems in Mechanical Engineering (IMS), Technical University Darmstadt

Otto-Berndt-Straße 2, 64287 Darmstadt, Germany

*E-mail: quurck@ims.tu-darmstadt.de

Abstract

Backup bearings (BB) limit the rotor translational movement during malfunction, overload or power loss in the active magnetic bearings (AMB) in order to enable safe spin down and reduce secondary damage. Especially for high speed applications like flywheels with high rotor inertia, the requirements towards the load capacity and service life of the BB is comparably high. For a special type of flywheel with exceptionally high speeds in the BB interface, a planetary BB system is presented. The planetary BB consists of multiple bearing units placed circumferentially around the stator. Its elastic properties are described as well as a contact damping approach. For cost efficient BB investigation, a scaled test rig is introduced and a parametric study of different delivitations simulations is done. Several quantification methods to evaluate severity, bearing loads and lifetime utilization during BB are presented and applied to the simulations.

The applicability of the planetary BB to vertical high speed rotors is confirmed by the simulation data and bearing element selection is affirmed. The results of the quantification methodologies show specific correlation to initial conditions and parameters like unbalance and in particular contact friction coefficient.

Keywords : backup bearing, flywheel, kinetic energy storage, lifetime, service life

1. Introduction

Flywheels for energy storage applications commonly use contact free magnetic bearings in order to reduce losses and maintenance. As most magnetically levitated rotors, flywheels need Backup Bearings (BB) for safety and availability. The task of the BB system is to limit the rotor translational movement during malfunction, overload or power loss in the active magnetic bearing (AMB) in order to enable safe spin down and reduce secondary damage. Advanced flywheels combine high inertia with high rotational speed to achieve maximum kinetic energy content and high energy density. This heightens the requirements for the BB system in terms of service life and load capacity. In a worst case scenario, the demanded service life of a flywheel BB corresponds to spin down times of several minutes.

In case of hollow cylinder shaped, hubless, outer rotor type (ORT) flywheel the rotor inertia and the surface speeds are comparably high. At the inner diameter, where the BB needs to be placed, more than 200 m/s occur, which is faster than most conventional shaft rotors. Special challenges of ORT BB are described by Quurck, et al. (2014) as well as the planetary BB system which was chosen for ORT flywheels. The planetary design was derived by the approach of Mohawk Innovative Technology, Inc. The use of multiple comparably small bearing units in each BB plain in circumferentially arrangement enables high surface speed operation and suppresses whirl motion.

2. Research objectives and approaches

The main aim of the BB research at the IMS is to find a suitable BB system for high speed ORT flywheels like the 1.5 kWh prototype “ETA290” with 290 mm inner diameter and a top speed of 14100 rpm. Furthermore, the investigation of the service lifetime and failure modes of the bearing components is targeted. Service lifetime denotes the number of rotor delevitations from a distinct dropping speed or how long the bearing can withstand without bearing failure or consecutive component damage during drop downs. To approach a robust and durable BB system for an ORT flywheel, the dynamic behavior of the rotor-stator interaction needs to be investigated. For this simulations are made in the state space simulation environment named ANEAS (Analysis of Nonlinear Active Magnetic Bearing Systems), which is implemented in MATLAB (Orth and Nordmann, 2002), (Orth, 2007).

As every model is a simplification and contains assumptions and uncertain parameters, experimental testing for verification needs to be done. Because full scale experiments of the planetary BB system with flywheels are expensive and bear uncalculatable hazards to machines and environment, in this paper a substitute rotor and stator as well as its planetary BB is used for simulation and later experiments. The simulation data is processed by different evaluation methods which are compared to each other. The results are used for design finalization of the test rig and further assessment of the planned experimental BB testing and shall be used for further flywheel development.

3. Test rig design

The function of the test rig is to mimic the dynamics of the ORT flywheel during rotor delevitation events (RDE), although the rotor is a conventional shaft rotor. Design criteria were similar bending eigenfrequencys and an identical ratio of polar and axial moment of inertia I_p/I_a. This ratio describes the gyroscopic properties of the rotor. As a specialty of the ORT flywheel the maximum surface speed of the BB should be reproduced by the test rig rotor. Further the rotor should be built from high strength steel with bigger mechanical and thermal robustness than the ORT flywheel made of fiber-reinforced plastic (FRP). After an iterative process, a modular and symmetric rotor design with exchangeable primary BB disc plains was found to fit the requirements best. Some properties of the original flywheel rotor "ETA290" and the test rig are given in Table 1. Fig. 1 shows a 3D model of the test rig rotor design and Fig. 2 shows a BB plain of the test rig consisting of the stator and 6 BB units. The test rig is planned to be set up in early 2017 and multiple RDEs in different BB configurations are intended.

Table 1 comparison of the flywheel and test rig rotor

feature	unit	ORT "ETA290"	test rig rotor
1st bending eigenfrequency	Hz	1152	1469
2nd bending eigenfrequency	Hz	1219	1851
inertia ratio	-	0.65	0.58
rotor mass	kg	149.4	18.1
max rotation speed	rpm	14100	21000
BB Diameter	m	0.29	0.21
max BB surface speed	m/s	243	230

The test rig rotor is magnetically suspended by two radial AMBs and driven by a permanent magnet (PM) synchronous machine. The axial levitation is done by an AMB sitting in between the two primary BB discs and is designed to levitate the rotor during RDEs in order to avoid axial contact. This is important because the ORT flywheels are axial levitated by PM bearings which are comparatively reliable and robust against external influence.

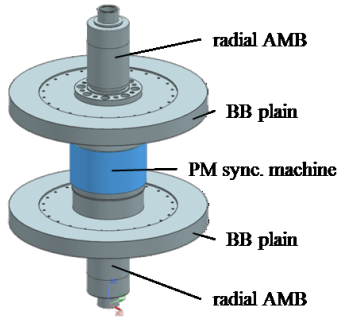

Fig. 1 3D Model of test rig rotor

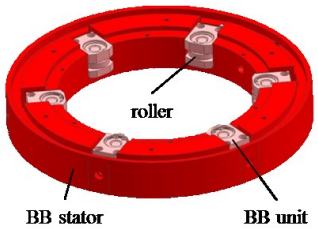

Fig. 2 Test rig planetary BB with 6 BB units with each two ball bearings and one roller

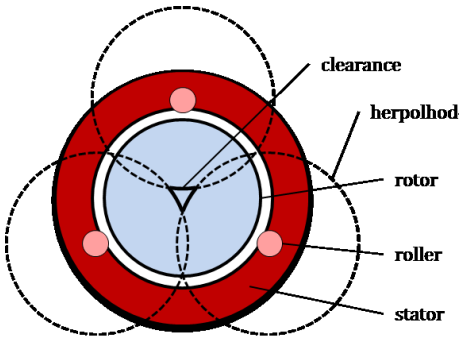

Fig. 3 Schematic illustration of the clearance build with 3 BB units

4. General modeling approach

Within ANEAS, discrete models of rotor and stator are transformed to state space models and reduced, whereby the eigenmodes of the uncoupled rotor and stator are truncated, which have small Hankel singular values and consequently do not contribute much to the global dynamic behavior of the system. Coupling between rotor and stator can be performed by the AMB and its controller dynamics, as well as through different types of BBs, like plain bearings and several types of rolling element bearings as well as the planetary BB design. All rolling element bearings use extra rotational degrees of freedom (DOF), and are fixed to translational DOF of the stator. The rotor-stator coupling in this

work results from the mechanical contact force and a negative radially symmetric stiffness of the PM synchronous machine. AMB forces are set to zero in order to represent a complete power loss. Due to the vertical orientation of the flywheel and test rig rotor, gravitation is neglected.

Both, rotor and stator are modelled with Timoshenko beam elements with 4 DOFs per node. The discretization of 31 elements at the rotor and 15 elements at the stator showed good agreement with a detailed 3D numeric modal analysis. Internal structural damping is considered by assuming 1 % modal damping.

The contact forces normally increase disproportional to the deflection, because they are caused by Hertzian contact elasticities of bearing components. To take this into account, nonlinear analytic calculation or experimentally generated force-deflection curves need to be regarded as well as a realistic contact damping model. The basic contact model is illustrated in Fig. 4 and explained in the following section. The complex multiple serial and parallel elastic model was simplified to a single DOF substitute elasticity with a suitable damping model, as illustrated in Fig 5.

4.1. Static elastic compliance of BB components

The nonlinear stiffness of the BB components determines the radial forces applied between rotor and stator and therefore their dynamics during RDE. For rolling element bearings the elastic compliance can be determined analytically with good accordance to measurements. Gargiulo (1980) gives a simplified analytic formula to calculate radial force F_{rad} in N for given bearing inner ring deflection δ of standard bearings using only the number of rolling elements Z, the rolling element diameter D_m and the contact angle β.

$$F_{rad} = 2.192e10 \frac{N}{m^2} \cdot Z \sqrt{D_r \cdot \delta^3 \cdot \cos^5 \beta} \tag{1}$$

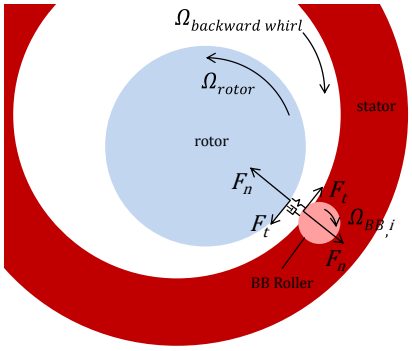

Fig. 4 Contact model used for simulation

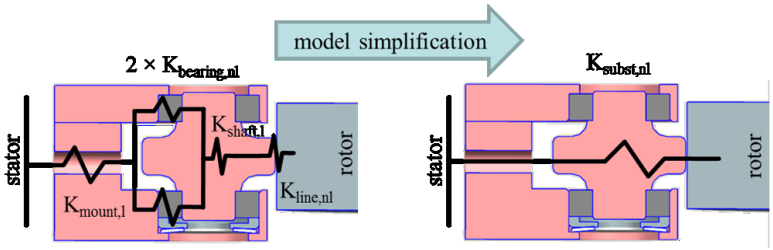

Fig. 5 Illustration of the discrete model of the elasticities of a BB unit. Left: parallel and serial elasticities. Right: simplified, nonlinear model used in simulation

For two parallel standard deep groove bearings of type 6001 with 8 balls each, in Fig. 6 a force deflection curve is shown, marked with the black pointed line. In the case of the planetary BB design multiple serial and parallel elasticities of a single BB unit have to be considered for an accurate calculation. Fig. 5 a vertical cross section of a BB unit is shown with an overlaid model of the discrete elasticities k_i. The index nl labels nonlinear and l linear characteristics. In order to reduce the complex elasticity to a single force deflection relation an experiment was performed in which the real elasticity of all present components in a realistic setup is represented. During the quasi-static experiment, the total deflection between a hardened steel plate and a bearing mount was recorded as well as the applied force. The measured force deflection curve in Fig. 7 is used further to determine the static force F_{static} lookup table in the simulation.

4.2 Contact damping

In case of nonlinear and impact like contact, situations a linear damping approach like $F_{damp} = d\dot{\delta}$ does not show a good accordance to real physical experiments. Especially negative contact forces, due to negative deflection velocities, shown in Fig. 6 as dashed blue line, disagree with mechanical realities. Another unrealistic feature of the linear damping approach is the discontinuous force at the beginning of the contact, where it is expected to be zero.

Microscopic plastic deformation and friction induced dissipative processes in the contact patches of impacting bodies can be macroscopically described by the coefficient of restitution. Hunt and Crossley (1975) created a modeling approach for impacting bodies which can describe vibro impacts with high accordance to experiments. The resulting

dynamic contact force F_{dyn} can be written as Eq. (2).

$$\boldsymbol{F_{dyn}(\delta, \dot{\delta}) = F_{static}(1 + 1.5\,\alpha\,\dot{\delta})} \tag{2}$$

The basic idea of this approach is to expand the pure elastic contact force approach using the damping coefficient α multiplied with deflection velocity. An energy dissipating hysteresis loop can be displayed when contact force is plotted over deflection in Fig. 6 in red solid line. The area enclosed by the loop quantifies the dissipation during contact. The approach of Hunt and Crossley delivers speed dependent, continuous, non-zero crossing contact forces and can be applied to different static elastic characteristics. In Fig. 6 exemplary simulations based on a static force deflection curve of Gargiulo is displayed and compared to linear damping and the Hunt & Crossley Model. Fig. 7 repeats the same with the static measured force-deflection curve of the BB unit mentioned in section above. This curve combined with the Hunt and Crossley contact damping approach with α = 5 s/m was chosen for further simulation.

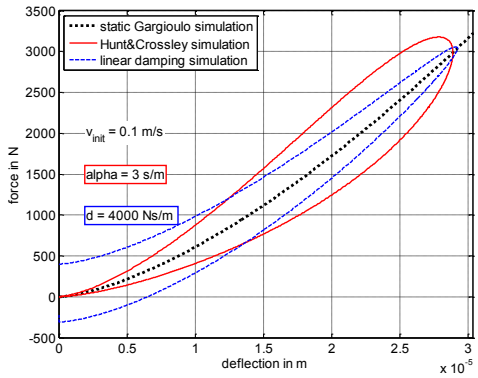

Fig. 6 calculated static and dynamic force deflection curves

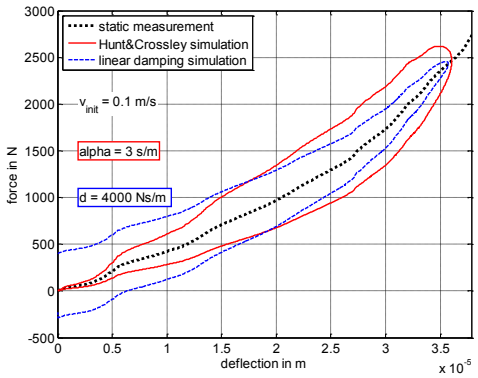

Fig. 7 measured static force deflection curve and different damping model applied

4.3 Friction

The rotation of the rotor leads to different surface velocities between BB interfaces. This relative velocity affects tangential friction forces during contact. This friction forces accelerate the rotational states of the BB units and decelerates the rotor's rotation. Simultaneously the friction forces affect the rotor's translational states. Typically the tangentially acting friction force causes backward whirl motions. Because of its dry character the assumption of Coulomb friction is an appropriate approach. In Eq. (3) a steady approximation of Coulombs friction law is given. It calculates the direction dependent friction force $\boldsymbol{F_{fric}}$ using the friction factor μ, the relative surface speed Δv and the normal force which was calculated before as the dynamic contact Force $\boldsymbol{F_{dyn}}$.

$$\mathrm{F_{fric}} = \mu \cdot F_{dyn} \cdot \left(\frac{2}{\pi}\arctan\left(100\,\frac{\mathrm{s}}{\mathrm{m}} \cdot \Delta \mathrm{v}\right)\right) \tag{3}$$

With viscous bearing lubrication the friction can be approximated by classical drag moment models described in bearing catalogs such as Schaeffler (2008). Eq. (4) gives the drag moment of one single bearing. It consist of a speed dependent part M_0 and a load dependent part M_1. This model was used in the presented simulation model.

$$\mathrm{M_{drag,BB}} = \mathrm{M_0} + M_1 \tag{4}$$

The values of M_0 and M_1 have to be calculated from manufacturer data and with the knowledge of the temperature dependent kinematic viscosity of the lubricant. The value was assumed to be $5\ \mathrm{mm^2/s}$ for simulation.

5. Planetary BB orbit

The planetary BB system has a noncircular clearance orbit which is defined by the enclosed area of the herpolhodes of the rotor touching the BB rollers. Fig. 3 illustrates the clearance orbit of the rotor in a BB system with only 3 rollers. The curvature of each section of the clearance orbit is defined by the sum of rotor and stator radius and represents the herpolhodes of the rotor touching the BB rollers. For simulation the curvature of the herpolhodes was neglected and simplified to straight lines. Connected to each other this straights form a polygon shaped BB orbit. The

noncircular BB orbit delivers different properties which have to be regarded. First of all, continuous contact during a whirl is prohibited because every change of polygon section results in a new impact, leading to bouncing rotor reaction. Former works from Helfert (2008) showed a whirl suppressing effect of deviation roller elements inserted in a conventional circular BB orbit. First tests confirm the jumping character of the rotor trajectory inside a planetary BB. The occurring backward whirl motion remained at low frequencies what can be explained by the soft and highly damped contacts of the BB units, compared to conventional BB bearings of that size. Simulation results confirm this assumption. However, high speed testing has to be performed to definitely confirm the general whirl resistance of a planetary BB system.

6. Evaluation of simulation results

Main interest of the simulation of RDE is the global dynamic behavior and the contact forces which may harm the rotor or the BB components. Therefore, simulation results contain all translational states of the rotor, its rotational speed, the tangential and radial forces of each BB unit and their rotational speed. Generally, RDEs deliver large amounts of data which have to be processed in a way that quantifies the severity of the RDE, the wear or the expected remaining service life of a bearing.

6.1 Position data based evaluation

One possibility is to evaluate the rotor's translational states in each BB plain. (Janse van Rensburg, 2015) proposes to calculate the length of the rotor trajectory normalized by the nominal air gap of the BB during a RDE. The dimensionless value is called D_{val}. Experimental testing showed interesting correlation between this normalized values and the occurring bearing wear during consecutive RDEs. Janse van Rensburg states this correlation with the continuous growing of inner friction inside the bearing.

6.2 Bearing load based evaluation

One other opportunity is to use the loads and rotational speeds of the BB. It is evident that these values can deliver more information about bearing wear than using only rotor states. As a downside of this approach the interpretation of these values may be more difficult, and experimental investigation with force and BB speed recording still needs to be done.

The easiest but most important force dependent assessment criterion, which needs no further interpretation, is the height of the maximum force peak during the RDE. To avoid plastic deformation this peak force needs to be lower than the static load C_0 rating of the used bearing.

The lifetime calculation of rolling element bearings following ISO 281 (2007) is supposed to calculate the number of revolutions at a defined load and rotational speed that a bearing can withstand at a certain failure probability. As failure mechanism the fatigue of steel interfaces is postulated. The fatigue is caused by the Hertzian contact stress of the rolling elements overrunning the raceway repeatedly during bearing rotation. The geometry, E-modulus and shear strength, of the contact partners as well as the number of rolling elements determine the sustainable load. For a desired failure probability of 10 % the number of revolutions multiplied by 10^6 is given by Eq. (5)

$$L_{10} = \left(\frac{C}{P_{eq}}\right)^p \tag{5}$$

The dynamic load rating of the bearing is C and P_{eq} stands for the applied equivalent load and the exponent p is a bearing type dependent constant. For ball bearings it is equal to 3.

Applied to the short, but very dynamic BB load the validity of the probabilistic fatigue model of the ISO 281 may be mistrusted in its original meaning. Especially the absence of thermal influences and realistic adjustment factors concerning varying lubrication and contamination will lead to deviations from experiments. Nevertheless, the calculated lifetime L_{10} corresponds to simulated or measured bearing loads, even if the calculated revolutions will not be exact. If the general assumption that a higher bearing load will lead to a lower lifetime comes true, low L_{10} values indicate RDEs with higher severity than RDEs with higher L_{10} values. Like D_{val} this offers the opportunity to compare different RDEs. Furthermore L_{10} may help to evaluate the appropriateness of the bearing selection for a certain system.

7. Parametric study

To apply the mentioned evaluation methods, a parametric study was performed with 35 simulations, each with a simulated time of 10 s. The simulations were grouped by five parameter sets, each with a single changed parameter. In each parameter set the starting rotational speed of the rotor n_0 was varied in seven steps from 4000 to 20000 rpm. For all simulations the starting position was 50% of the radial air gap of 0.42 mm. The rotor was released with a defined starting velocity v_0 in backward whirl direction, what lead to the most critical RDEs. In order to evaluate the sensitivity to staring conditions and parameters, like translational starting velocity v_0, friction factor μ and total unbalance U, these parameters were changed in one parameter set for all seven associated simulations. In Table 2 the used parameters are listed.

Table 2 Parameters for 5 different parameter sets. Only the changed parameter is mentioned. No entries indicate that the value of the reference set was used.

parameter set name		reference	2U	0.5U	$10v_0$	μ=0.1
starting velocity v_0	m/s	0.01			0.1	
total unbalance U	kg m	5.62×10^{-5}	1.12×10^{-4}	2.81×10^{-5}		
friction coefficient μ	-	0.15				0.1

For illustration purposes, simulation data of the reference parameter set and a starting rotational speed of 20000 rpm is presented. The rotor position in the upper BB is displayed in Fig. 8. In Fig. 9 the translational velocity is plotted over time. In Fig. 10 the corresponding contact normal force, which is applied to the rotor, is displayed. The position plot shows that most of the time the rotor is near or contacting the BB, while the center of the BB orbit is passed comparably rarely. During contact the rotor position is displayed outside the polygon. Induced by the tangential friction force the translational rotor movement is a clockwise backward whirl. The normal contact force shows distinct phases where no contact occurs, what indicates that the rotor performs no continuous rolling in the BB clearance orbit. The contact force also indicates two phases where high force peaks occur. During these phases the rotor performs its highest translational speeds of around 0.2 m/s. During these two phases the BB units were mainly accelerated to the synchronous speed, while the rotor loses 7 % of its rotational speed in 1 s. After this friction intensive phase the rotor translationally slows down and normal forces decreases simultaneously. The rotational speed of BB units and rotor after synchronization decreases by 3% in 9 s. In all 35 simulations this global behavior can be found. Differences were basically registered in the height of forces and velocities and the times when synchronization takes place. No synchronization after 3 s could be registered, which means that the first 3 s appear to be most crucial for the BB loads.

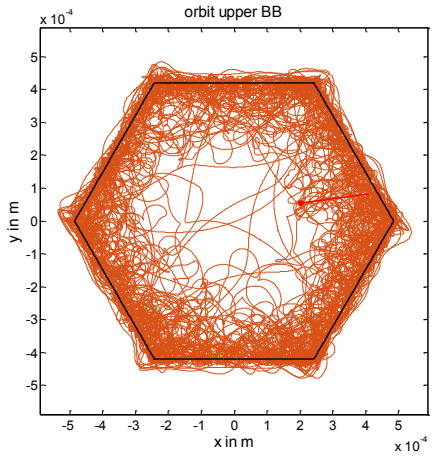

Fig. 8 Rotor position in upper BB plain during a 10 s RDE

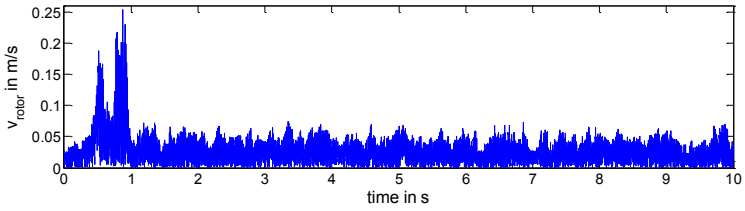

Fig. 9 Translational rotor velocity rotor in upper BB plain

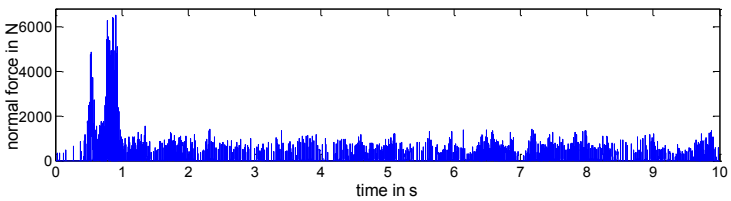

Fig. 10 Normal contact force applied to the rotor

8. Results

The evaluation results of the 35 simulations are plotted over the rotational speed at simulation start in Fig. 11 to 14. First of all the maximum force F_{max} was assessed to evaluate plastic deformation. As can be seen in Fig. 11 in almost every simulation set, F_{max} rises with an increase of rotor speed. In parameter set 2U the highest loads occur while 0.5U tend to the lowest loads. An increased staring velocity does not increase F_{max}. In Fig. 12 the total revolutions of a BB unit during a simulation divided by the L_{10} lifetime is displayed. The analysis was done for the BB unit with lowest ratio in order to emphasize the most critical unit. This ratio can be interpreted as lifetime utilization value. The higher the calculated value is, the more likely a bearing failure is. In other words, it can be assumed the higher a value is, the more the bearing is worn due to the simulated RDE. Initial translational speed v_0 does not to have a significant influence on the results. A detailed analysis shows that after few impacts, the translational velocity develops independently from the initial contact. Same counts for the influence of the unbalance. Although the height of the unbalance seems to affect contact forces, but the correlation between both is comparatively low. The contact friction factor μ has a very high influence. In the low friction parameter set μ=0.1, the maximum contact force is reduced by roughly 50 % to the averaged values of the other simulations. Also the lifetime utilization value shows significantly lower values.

Of particular interest is how the D_{val} values correlate with the L_{10} values. Fig. 13 and Fig. 14 show both values for all simulations. D_{val} is very sensitive against different parameters; especially the height of the unbalance influences the results. With rising RDE speed D_{val} tends to higher values what indicates higher rotor movements and therefore dynamic loads. Because the unbalance causes natural circular movement of the rotor, the correlation towards D_{val} can be explained. To interpret D_{val} the unbalance has to be regarded especially because RDEs can also be caused by a sudden change of unbalance, or during RDEs the unbalance can change in cause of mechanical deformations.

Examining L_{10} values, the correlation towards starting speed is more significant compared to unbalance and v_0. Interesting results can be observed by the comparison of the low friction parameter set. While D_{val} indicates higher rotor movement and therefore higher bearing wear can be interpreted, the L_{10} values indicate lower bearing loads and longer lifetime. This coherence needs to be investigated further and experimental testing will deliver more insight to the actual correlations.

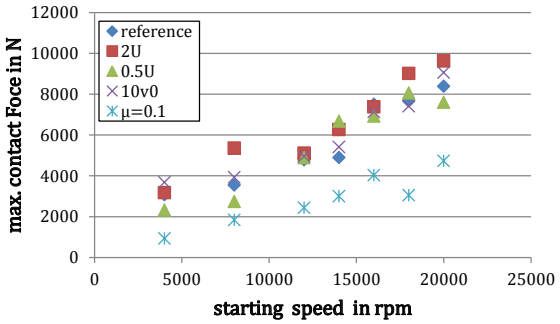

Fig. 11 Maximum contact force peak during simulations

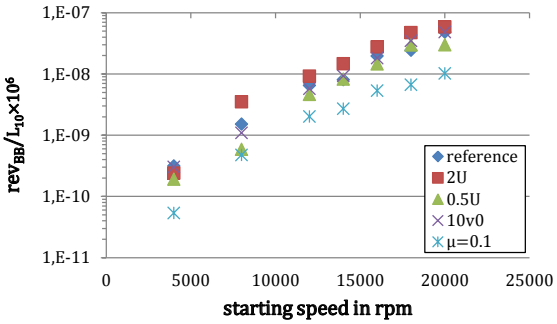

Fig. 12 Total revolutions of the most critical BB unit divided by calculated L_{10} lifetime

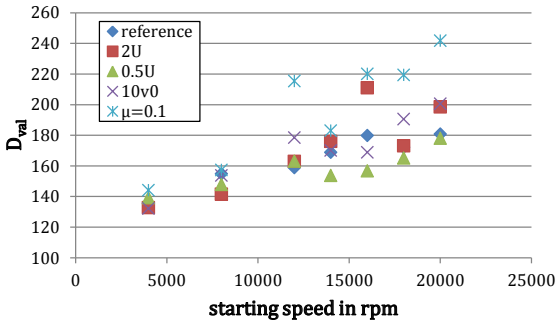

Fig. 13 D_{val} after 10 s simulations

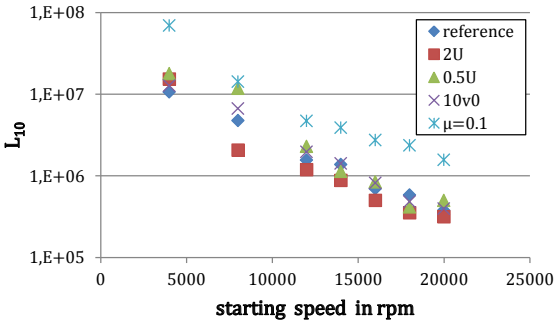

Fig. 14 L_{10} value after 10 s simulations

9. Conclusion

The work showed different ways to quantify the severity of RDEs using force, rotational BB speeds and position data. In the design phase especially the force dependent quantification data helps to assess dynamic simulations and can give information about the selection and design of BB components. The used modeling and simulation environment of ANEAS can deliver the necessary simulation data for conventional and the planetary BB design approaches. The simulation data of the planetary BB showed non-problematic RDE characteristics and controllable bearing forces. An important result for the development of planetary BB is that the contact friction factor needs to be as low as possible in order to lower translational rotor velocities and therefore bearing loads, even though the synchronization between BB and rotor takes more time. The material selection or coating of the BB interfaces therefore is an important design aspect especially when very high surface velocities are considered.

The results of the parametric study show significant correlation to initial conditions and parameters of the simulation model. Maximum contact forces as well as the ratio of BB revolutions and calculated L_{10} values can indicate lifetime utilization during RDEs, even if the calculation does not meet exact BB lifetime because of unknown adjustment factors and failure modes that do not result from surface fatigue, postulated in the ISO 281.

10. Outlook

First of all, the showed test rig needs to be set up and put into operation. Then the accordance of the simulation data needs to be verified. The experimental testing is going to deliver information about bearing wear, actual load capacity and service life of BB systems. To evaluate the frictional energy dissipation during RDEs the test rig will be equipped with thermal sensors and speed sensors for the rotational BB unit states.

The planetary BB needs to be adapted to the upcoming ORT flywheel prototypes and experimentally tested to assess the validity of the test rig results. Generally, it is planned to find a way to assess any BB system by simulation to determine an appropriate BB system. Being able to predict service life of the system without further expensive BB testing of the original rotor is the next goal.

References

Gariulo, E.P., A simple way to estimate bearing stiffness, Machine Design 52 (1980), pp. 107-110

Helfert, M., Rotor delevitaions in rolling element bearings – experimental investigation of rotor-backup bearing-contact, (in German), PhD. thesis, Darmstadt (2008)

Hunt, K., Crossley F., Coefficient of restitution interpreted as damping in vibroimpact, Transactions of the ASME, Journal of Applied Mechanics, pp. 440-445, (1975)

International Standardization Organisation, ISO 281:2007 Rolling bearings - Dynamic load ratings and rating life (2007)

Janse van Rensburg, J.J. et al., Backup-Bearing lifetime prediction using quantified delevitation severity indicators, Proceedings of Workshop on Magnetic Bearing Technology 10, (2015)

Mohawk Innovative Technology, Inc., Auxiliary Bearing Developed for 140 mm Shaft with 1000 Pound Load at 18,000 RPM!, MiTi Developments, Vol 8, (1999)

Orth, M., Backup Bearing contact of magnetically suspended rotors (in German), Ph.D. thesis, Shaker Aachen, (2007)

Orth, M. Nordmann R., ANEAS a modeling tool for nonlinear analysis of active magnetic bearing systems, 2nd IFAC Conference on Mechatronic Systems, Berkley, USA, pp. 357-362, (2002)

Quurck, L. Schaede, H. Richter M. Rinderknecht S., High Speed Backup Bearings for Outer-Rotor-Type Flywheels – Proposed Test Rig Design, Proceedings of ISMB14, (2014)

Schaeffler, Wälzlager, manufacturer catalog, pp. 64 (2008)